Strojniški vestnik - Journal of Mechanical Engineering 58(2012)10, 563-570
DOI:10.5545/sv-jme.2009.085
Paper received: 2009-07-13, paper accepted: 2012-07-12

Manipulability of a Haptic Mechanism within the Cylindrical Space of an MR Scanner

Matej Rajh[1,*] – Srečko Glodež[2] – Jože Flašker[3] – Karl Gotlih[3]
[1] Rajh Plus d.o.o., Slovenia
[2] Faculty of Natural Science and Mathematics, University of Maribor, Slovenia
[1] Faculty of Mechanical Engineering, University of Maribor, Slovenia

The aim of this paper is to present developed 3 DOF haptic mechanism and 3D visualization method for analysis of mechanism manipulability problems within limited space. Improvement in mechanism manipulability within cylindrical space is crucial for devices, which operate in MR tunnel. This solution enables the plotting of quantitative 3D representation for each point in the mechanism's workspace, using selected resolution which can be determined in advance. The cross-section between the limited space and the whole arbitrary workspace shows the ability for movement execution.
Key words: manipulability, Jacobian matrix, workspace, haptic mechanism, MR compatibility, limited workspace

0 INTRODUCTION

The choice of a robotic mechanism depends on the task or the type of work to be performed and is determined by the positions of the robots, their dimensions, and structure. In general, this selection is done through experience and intuition; therefore, it is important to formulate a quantitative measurement for the robotic system's manipulation capability, which can be useful during robot control and in trajectory planning. In regard to this perspective, Yoshikawa proposed the concept of kinematic manipulability measurements as described in [1].

Magnetic resonance (MR) compatible haptic devices have certain special structural and operational properties because of the magnetic field and MR scanner shape. A few papers relating to this problem have been published recently ([1] to [4]). Dovat et al. described a mechanical interface to use in conjunction with functional magnetic resonance imaging (fMRI). Two designs were retained and implemented from MR compatible materials. They suggested that simpler interfaces using potential mechanical energy can produce position dependent force fields during arm movements, and can be used to study the brain mechanisms. In another paper from Dovat et al. was presented a 2 degrees of freedom (DOF) haptic interface, which is driven by hydrostatic transmission separated into a master and an MR compatible slave system. Khanicheh et. al. presented the design, fabrication and preliminary testing of a novel, one degree of freedom, MR compatible, computer controlled, variable resistance hand device that may be used in brain MR imaging during hand grip rehabilitation. A novel feature of the device is the use of Electro-Rheological Fluids (ERFs) to achieve tunable and controllable resistive force generation. Moreover, the development of the first magnetic resonance imaging (MRI)-compatible robotic system capable of automated brachytherapy seed placement was introduced by Muntener et. al.

However, the above quoted papers do not consider the manipulability of MR mechanisms as one of the most significant design attributes for quality force transmission in haptic interfaces when considering a limited working space. This can play an important role in the mechanism's design because operation close to the singularity point could lead to serious operating problems. Only rare articles ([5] and [6]) are involved in the area of manipulability analyses in haptic devices, but they do not include the particularity of limited space and MR compatible mechanisms. In addition, when we talk about operation within a limited workspace any manipulability problem becomes more complex and any improvements in mechanism design or the position of the mechanism's base could be even more significant.

In this work, the limited workspace is presented by a block placed inside the MR scanner bore with cross-section of 200×350 mm or with the diagonal length equal to human forearm as shown in Fig. 1. The main constraint of this workspace is its very high density of magnetic field. For this reason, safety is crucial during the robot operation within an MR environment exposed to a strong magnetic field of 1.5 to 3 T.

The robot, must therefore, be insensitive to the imaging sequence and should not disturb the imaging itself. Functional magnetic resonance imaging scanning sequences are even more sensitive to inhomogenities of the magnetic field than MRI sequences [7] to [9].

*Corr. Author's Address: Rajh Plus d.o.o., Črešnjevec 143, 2310 Slovenska Bistrica, Slovenia, matej.rajh@rajh.eu

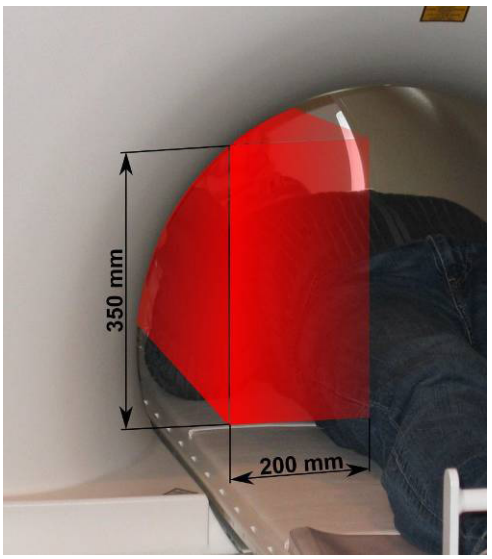

Fig. 1. *Red colour indicates the task space inside the MR tunnel*

The main aim of this work was to design a new 3DOF fMRI compatible haptic mechanism that can be driven by electric motors, despite usually being banned from the MR environment. However, the motors have excellent control possibilities. Some unique changes have been made in mechanism design, which become reasonable when considering the mentioned structural and geometrical limitations.

A kinematic model to optimize mechanism characteristics has been proposed to provide good manipulability of the mechanism and clearly present dexterity properties. The model visualizes manipulability characteristics in the tunnel of the MR device and enables the interpretation of possible improvements in sections of the volume.

1 MR COMPATIBLE HAPTIC MECHANISM

1.1 Haptics

An haptic interface is a force feedback device, which enables its user to interact with a virtual world or a remote environment explored by a slave device. It aims at matching the force and displacements given by the user and those applied to the virtual world. Such systems are in growing demand for applications such as force feedback remote-control systems for extreme environments, man-machine interaction, training in professional operating procedures and rehabilitation ([10] to [16]).

Usually, haptic interfaces make use of a mechanically actuated structure whose distal link is equipped with a handle. When manipulating this handle to interact with the explored world, the user feels the apparent mass, compliance and friction of the interface. This distortion introduced between the operator and the virtual environment must be identified in order to enhance the design of the device and develop appropriate control laws. The device's workspace should be large enough to cover or exceed the required workspace. Furthermore, a compromise is needed between the haptic device workspace size and the available output forces [16]. In order to reach good "virtual feeling" transmissions, the device must move very easily. Ideally, weight, friction, backlash, slip, material deformations etc would be absent. Therefore, good manipulability is also very important.

1.2 MR Compatibility and Choice of Materials

Over the past few years, fMRI has established itself as a major research tool for investigating the brain mechanisms of motor control and cognition. Performing arm movements in controllable dynamic environments during fMRI could provide important insights into human motor control and related dysfunctions, and enable therapists to quantify, monitor, and improve physical rehabilitation [1] to [3], [17].

The major problem when creating fMRI compatible robots is the strong magnetic field needed for MRI (1.5 to 3 T) precluding the use of conventional materials or actuators close to the scanner bore. This requirement prevents the use of conventional robotic interfaces. MR environment refers to the general environment near an MR scanner. In particular, it includes the area encompassed by the 10 mT line. This may or may not include the entire magnet room and surrounding support areas [18].

By referring to the device design criteria for fMRI environment introduced by Hartwig et al. [18], we decided that this new mechanism would be composed of composite materials, ceramic passive mechanical devices and ropes from high strength polymer fibres.

Carbon and advanced ceramics fit well within the MR environment even inside an MR tunnel [19]. Plastics are easily machined but do not have the strength needed to build a light structure with low inertia. Non-ferrous metals (Aluminium, Beryllium, Copper, etc.) are desirable for their non-magnetic properties and strength. Non-ferrous metals may contain some impurities, which would cause certain magnetic properties. Heating and stress to the structure may also introduce some undesirable magnetic properties and could cause some artifacts within an image [20].

The main problem with composites, high strength fibres and ceramic mechanical elements is their cost, availability of elements, and lack of appropriate data regarding exact mechanical properties.

Another problem besides image artefacts is radio-frequency (RF) noise. It often appears as static on the image and can be caused by an electrical device located anywhere in the MR procedure room. Some members of our work group conducted an experiment on the same fMRI scanner using a reshaped Phantom haptic device [12], which was far enough from the scanner bore and had a lengthened handle for MR influence exclusion. The exact results have not yet been published, but this experiment did not show any influence on image quality.

2 KINEMATIC DESIGN OF THE PROPOSED MECHANISM

2.1 Kinematic Requirements

When operating in an MRI tunnel, it is quite difficult to decide which mechanical structure is appropriate because the workspace is limited and it is impossible to incorporate a parallel mechanism with a high level of stiffness. On the other hand, according to Lee and Lee [21], serial manipulators are unsuitable for haptic devices, because of low level stiffness. Therefore, we searched for a combined mechanism, which had to be driven on its base and with actuators mounted away from the tunnel, as far as possible. It is for this reason that MR compatible haptic devices are mostly developed as a 2DOF devices [1] to [3], [9], [22] and [23].

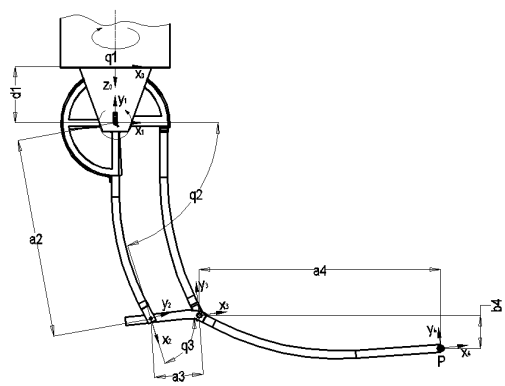

Fig. 2. *Schematic view of curved haptic mechanism*

A schematic view of the treated haptic mechanism is shown on Fig. 2, where "0" indicates global coordinate system and P (Eq. (1)) is the position at the top end of the mechanism. It was derived using Denavit-Hartenberg parameters [24]. The mechanism has following dimensions: d_1 =140 mm, a_2 = 470 mm, a_3 = 115 mm, a_4 = 565 mm, b_4 = –80 mm.

$$P = \begin{bmatrix} p_x \\ p_y \\ p_z \end{bmatrix} = \begin{bmatrix} C_1\left(a_2C_2 + \left(a_3 + a_4\right)C_{23} - b_4S_{23}\right) \\ S_1\left(a_2C_2 + \left(a_3 + a_4\right)C_{23} - b_4S_{23}\right) \\ d_1 - b_4C_{23} - a_2S_2 - \left(a_3 + a_4\right)S_{23} \end{bmatrix}, \quad (1)$$

with $S_i = \sin(q_i)$, $C_i = \cos(q_i)$, $C_{ij}=\cos(q_{ij})$, $S_{ij}=\sin(q_{ij})$ and $q_{ij}= q_i+ q_j$.

2.2 Mechanism Design

The kinematical background as described previously can serve as a basis during the design process of a treated haptic mechanism and also for its final production and exploitation in a MR compatible haptic interface. An important problem to be solved is how to ensure that the mechanism is as efficient as it is in an open space. In order to do this, the shape of the mechanism and handle must be carefully designed. The mechanism consists of four bars with innovative curved shapes, as shown on Fig. 2, that assure accessibility to each experimental point in the MR tunnel, high stiffness and good manipulability characteristics. The shape is adapted to the tunnel of the MRI scanner. So far, an aluminium mock-up has been built for verification of kinematic suitability (Fig. 3). Moreover, this same mechanism can be upgraded with drives and controls to test a full haptic performance. For the prototype are used Maxon DC motors and special haptic controls developed by Laboratory for Robotics at the Faculty of Electrical Engineering in Ljubljana.

Fig. 3. *Manufactured aluminium mechanism used for kinematic tests*

The mechanism is composed of two main segments, which are driven by a capstan or cable drive, which is the most widely used driving solution in haptic devices due to its low backlash (almost zero), stiffness, backdrivability and simplicity [12], [16], [25] and [26]. Backdrivabililty is a measure of how accurately a force or motion applied at the top end is reproduced at the input end.

In a mechanical robot-like linkage, good backdrivability means that a person can grasp the tip of the linkage and move it around effortlessly [16]. Fig. 4 shows the placement of a complete mechanism within a MR environment and its position in regard to the patient.

3 MANIPULABILITY

In the literature manipulability is originally defined as a measure of a robotic structure's performances, normally given in the force domain by means of manipulability ellipsoids or polytopes [5]. The manipulability index proposed by Yoshikawa [27] is defined by the following equation:

$$w = det\left(J\right), \tag{2}$$

which represents the volume of the velocity ellipsoid.

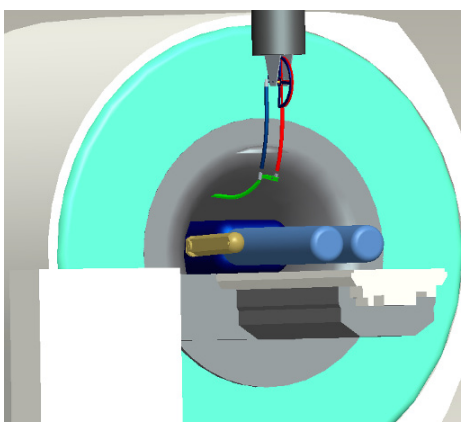

Fig. 4. *The model of MRI device with patient and mounted mechanism*

Close to the singularity point the volume of the ellipsoid is still large and imprecisely reflects the closeness of singularity because the parameter is not sensitive enough. This is the main reason for the shortest ellipsoid axes being used as the quantitative measurement of the closeness of a manipulator to singularity.

A haptic device should have excellent mobility to facilitate the operator giving orders. In addition, the generation of force and moment along a certain direction should be done easily in order to deliver a precise force to the operator. Therefore, it is necessary to ensure consistent manipulability characteristics within the workspace [21] and [28].

The velocity and force transmission characteristics of a manipulator at any posture can be represented geometrically as ellipsoids (Fig. 5). The velocity ellipsoid is a useful tool for visualizing the velocity transmission characteristics of a manipulator at a specific posture.

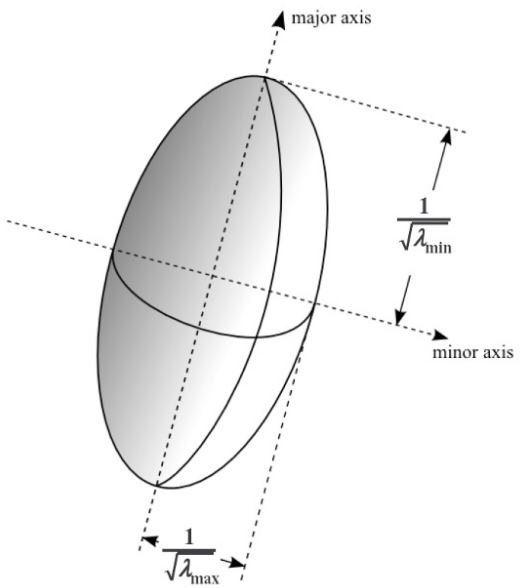

Fig. 5. *Velocity ellipsoid with principal axes*

Consider n-degree of freedom manipulator with configuration space coordinates q (internal coordinates), with $q_i \in \Re^n$, and a task described by the vector $\mathbf{x}$, $x_j \in \Re^m$, and $m \leq n$. The geometric transformation from configuration space to task space (external coordinates) is:

$$\mathbf{x} = \mathbf{x}\left(\mathbf{q}\right). \tag{3}$$

Differentiating $\mathbf{x}$ with respect to the time, we obtain:

$$\dot{\mathbf{x}} = J\dot{\mathbf{q}}, \tag{4}$$

where J is the $m \times n$ Jacobian matrix which can be obtained as follows:

$$J = \frac{\partial \mathbf{x}}{\partial \mathbf{q}}, \tag{5}$$

and consequently for our mechanism according to Eq. (8).

The Jacobian is simply a linear transformation that maps the joint velocity in $\Re^n$ into task velocity in $\Re^m$. The unit sphere in $\Re^n$ is defined by:

$$\left\|\dot{\mathbf{q}}\right\|^2 = \dot{q}_1^2 + \dot{q}_2^2 + \cdots + \dot{q}_n^2 \leq 1, \tag{6}$$

and is mapped into an ellipsoid in $\Re^m$ defined by:

$$\dot{\mathbf{x}}^T \left(JJ^T\right)^{-1} \dot{\mathbf{x}} \leq 1. \tag{7}$$

The principal axes of the velocity ellipsoid coincide with the eigenvectors of $(JJ^T)^{-1}$ and the length of a principal axes is equal to the reciprocal of the corresponding eigenvalue's square root [29].

$$J = \begin{bmatrix} -S_1\left(a_2C_2 + \left(a_3+a_4\right)C_{23} - b_4S_{23}\right) & -C_1\left(b_4C_{23} + a_2S_2 + \left(a_3+a_4\right)S_{23}\right) & C_1\left(b_4C_{23} + a_2S_2 + \left(a_3+a_4\right)S_{23}\right) \\ C_1\left(a_2C_2 + \left(a_3+a_4\right)C_{23} - b_4S_{23}\right) & -S_1\left(b_4C_{23} + a_2S_2 + \left(a_3+a_4\right)S_{23}\right) & S_1\left(-b_4C_{23} - \left(a_3+a_4\right)S_{23}\right) \\ 0 & -a_2C_2 - \left(a_3+a_4\right)C_{23} - b_4S_{23} & -\left(a_3+a_4\right)C_{23} + b_4S_{23} \end{bmatrix}. \tag{8}$$

A vector **v**, with its origin in the centre of the velocity ellipsoid (TCP – tool centre point, which is equal to the top of the mechanism in our case) and magnitude equal to the length from the ellipsoid centre to a point on the surface of the ellipsoid, represents the velocity vector in this particular direction. If the length of the vector is equal in all directions this mechanism posture is isotropic. In this case, the velocity ellipsoid is a sphere. In some particular mechanism postures, the ellipsoid loses one of its dimensions. The ellipsoid degenerates into an ellipse. These particular postures are the singular postures of the mechanism. In the cases of these singularities, the TCP can only move in directions within the plane of the ellipse.

The velocity ellipsoid indicates the manipulability of the manipulator in any posture. The highest manipulability is obtained in the direction of the longest principal axes of the ellipsoid. The lowest manipulability is in the direction of the shortest principal axes.

The robot's working space is velocity anisotropic [30]. This fact restricts the working space to a subset where the required TCP velocities can be performed and others where the required velocities can not be obtained.

The parameter for measuring the manipulability of the robot in any posture is the shortest length of the principal axis of the velocity ellipsoid. If the length of the shortest principal axis at a point within the working space is long enough, the robot will be able to perform the required manipulability, and the robot's posture and the corresponding point are acceptable. If not, this point within the working space is unacceptable.

The optimal direction for effecting velocity is along the major axis of the ellipsoid, where the transmission ratio is at a maximum. Conversely, the velocity is most accurately controlled along the minor axis of the ellipsoid, where the transmission ratio is at a minimum. Velocity is the most accurately controlled in the direction where the manipulator can resist large disturbance forces, and force is most accurately controlled in the direction where the manipulator can quickly adapt its motion [16] to [18], [21], [23] to [25], [28] and [31].

4 VISUALIZATION OF MANIPULABILITY INDICES

4.1 3D Representation of Manipulability

A computational model was developed, within the framework of the presented research which is able to analyze the manipulability properties of the mechanism with a predefined Jacobian matrix. Volumetric representation of the manipulability index is used for the representation of calculated data.

In the developed model, the mechanism workspace is discretised. An equidistant mesh of points is a substitute for the whole set. The manipulability of the mechanism at each point of the mesh has a scalar value between 0 and 1 and is defined as the shortest axis of the velocity ellipsoid. A value for manipulability index of 1 means that the mechanism has the highest manipulability at the treated discretised point. If the value is 0, the mechanism has a singular position.

To find the best position for task space within the mechanism's workspace, the algorithm moves the task space through a set of discrete points within the workspace. At each position it counts the number of points regarding the mechanism's workspace that

are located within the task space. From all possible positions, it chooses the position within task space that has the highest number of counted points with adequate manipulability.

4.2 Graphical Manipulability Analysis within a Limited Space

When a human moves the mechanism handle inside the tunnel it is very important that there is the possibility to adapt the best dexterity characteristics within the area where the movements are to be performed. Therefore, this method is very useful for the adaptation of a mechanism's base position when the task changes. The operator can quickly define a new optimal position, obtain better force transmission, and more accurate results.

4.3 Results

The developed program is able to show the mechanism's workspace (Fig. 6) and appurtenant indices of manipulability within an open space or indices in a predefined limited workspace (Fig. 7). In the case of an MRI scanner, the entire workspace is half of a cylinder with 60 cm diameter, but it is usually reduced to the task space. Tests for different shapes were also performed, mainly for sphere and block and showed great results for arbitrary shapes.

The lowest manipulability index in the useful area of MR tunnel is 0.5, such a high value indicates that the mechanism's design is appropriate for haptic applications. In this particular case, there are 21 slice planes (Fig. 7) and the best plane from the manipulability point of view is plane number 16 (Fig. 7).

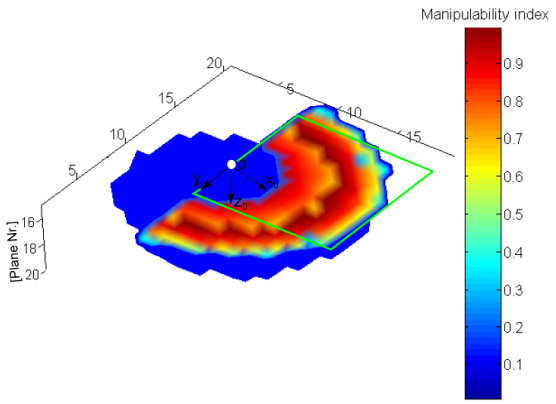

Fig. 6. 3D-plot of manipulability indices in an open workspace at slice plane 15 of 21 (the white point indicates the origin coordinates of the mechanism and the green frame indicates limited space)

Every task of a patient's hand movements has different requirements and positions inside the tunnel. With the help of 3D graphical representation, it is possible to evaluate manipulability characteristics in different positions, thus enabling the user to adapt the mechanism's base position according to a direction for better manipulability index.

5 CONCLUSIONS

A new mechanism as a force-feedback device to be used for evaluating brain activation by movements

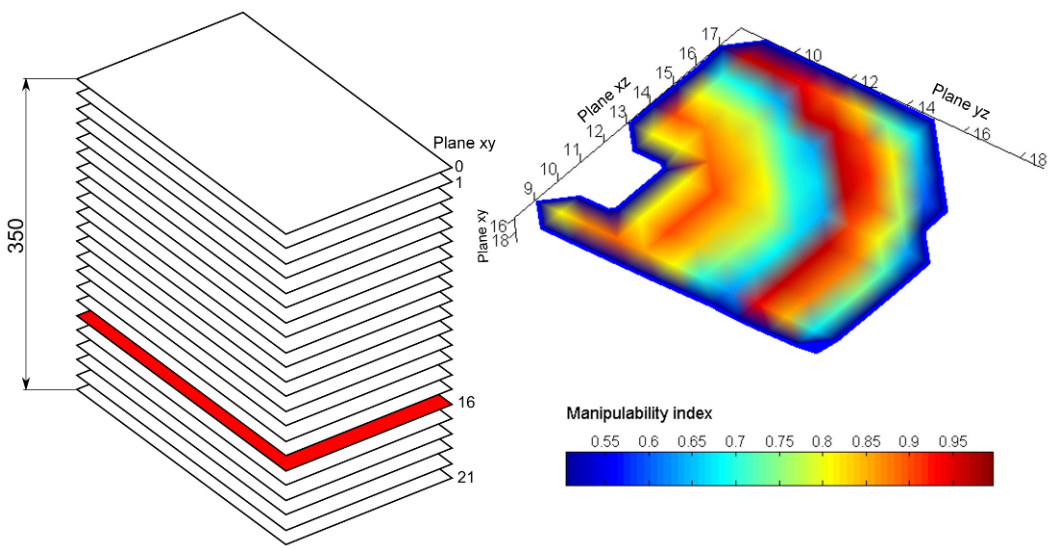

Fig. 7. *Slice planes of workspace (left) and 3D-plot of manipulability indices in limited workspace of MR tunnel (slice plane xy - number 16)*

of a human's upper extremity has shown good manipulability properties inside a limited space. This mechanism should be installed within an MR environment and for this reason it has to be MR compatible and all its active mechanical elements placed outside the critical zone using an outstandingly high density of magnetic field.

Low inertia and the ability to move very easily are the main design requirements owing to their haptic functions. Low inertia is achieved by using a light structure and high strength materials. On the other hand, it is easy to move the mechanism because of manipulability optimization. The method of 3D representation is very useful for imaging the properties of different placements of the mechanism within a limited space. It helps us to reach better mechanism positions and assures higher manipulability indices inside the workspace of the MR tunnel.

The developed computer program is also useful as a design tool for robot production cells as it enables better insight into workspace or more efficient use of workspace. The aim of our work in the future is the development of user friendly interface for production cells and haptic interface design, and their off-line programming by considering optimal manipulability characteristics. Additional work can also be done on the export of 3D plots in different CAD formats, thus providing the possibility of importing workspaces with common manipulability indices into all major PLM systems.

6 ACKNOWLEDGEMENTS

The authors thank professor Marko Munih and Aleš Hribar for their advice in the area of haptic mechanisms and MR compatibility, and all the staff at the University Medical Centre Ljubljana for enabling the testing of the mechanism's mock-up.

7 REFERENCES

[1] Dovat, L., Gassert, R., Chapuuis, D., Ganesh, G., Burdet, E., Bleuler, H. (2005). A haptic interface based on potential mechanical energy to investigate human motor control using fMRI. *Proceedings of the IEEE Engineering in Medicine and Biology, 27th Annual Conference Shanghai*, p. 5021-5024.

[2] Khanicheh, A., Muto, A., Triantafyllou, C., Weinberg, B., Loukas, A., Tzika, A., Mavroidis, C. (2006). fMRI-compatible rehabilitation hand device. *Journal of NeuroEngineering and rehabilitation, BioMed Central*, vol. 24, no. 3.

[3] Gassert, R., Dovat, L., Lambercy, O., Ruffieux, Y., Chapuis, D., Ganesh, G., Burdet, E., Bleuler, H. (2006). A 2-DOF fMRI compatible haptic interface to investigate the neural control of arm movements. *Proceedings of the IEEE International Conference on Robotics and Automation*.

[4] Muntener, M., Patriciu, A., Petrisor, D., Mazilu, D., Bagga, H., Kavoussi, L., Cleary, K., Stoianovici, D. (2006). Magnetic resonance imaging compatible robotic system for fully automated Brachytherapy seed placement. *Urology*, vol. 68, no. 6, p. 1313-1317.

[5] Gallina, P., Rosati, G. (2002). Manipulability of a planar wire driven haptic device. *Mechanism and Machine Theory*, vol. 37, no. 2, p. 215-228, DOI:10.1016/S0094-114X(01)00076-3.

[6] Kwon, T.B., Song, J.B. (2006). Force display using a hybrid haptic device composed of motors and brakes. *Mechatronics*, vol. 16, no. 5, p. 249-257, DOI:10.1016/j.mechatronics.2005.12.003.

[7] Hribar, A., Koritnik, B., Munih, M. (2009). Phantom haptic device upgrade for use in fMRI. *Medical and Biological Engineering and Computing*, vol. 47 p. 677-684, DOI:10.1007/s11517-009-0462-z.

[8] Hribar, A., Munih, M. (2010). Development and testing of fMRI-compatible haptic interface. *Robotica*, vol. 28, no. 2, p. 259-65, DOI:10.1017/S0263574709990646.

[9] Burdet, E., Gassert, R., Gowrishankar, G., Chapuis, D., Bleuler, H. (2006). fMRI compatible haptic interfaces to investigate human motor control. *Proceedings of 9th International Symposium on Experimental Robotics*,p. 25-34, DOI:10.1007/11552246_3.

[10] Payandeh, S., Dill, J., Zhang, J. (2007). Using haptic feedback as an aid in the design of passive mechanisms. *Computer-Aided Design*, vol. 39, no. 6, p. 528-538, DOI:10.1016/j.cad.2007.01.011.

[11] Hirabayashi, T., Akizono, J., Yamamoto, T., Sakai, H., Yano, H. (2006). Teleooperation of construction machines with haptic information for underwater applications. *Automation in Construction*, vol. 15, no.5, p. 563-570, DOI:10.1016/j.autcon.2005.07.008.

[12] Selected OEMs & System Integrators of SensAble Products (2008). Retrieved at 2008-12-18, from *http://www.sensable.com/oems-integrators.htm.*

[13] Wang, P., Becker, A.A., Jones, I.A., Glover, A.T., Benford, S.D., Greenhalgh, C.M., Vloeberghs, M. (2006). A virtual reality surgey simulation of cutting and retraction in neurosurgery with force-feedback. *Computer Methods and Programs in Biomedicine*, vol. 84, no. 1, p. 11-18.

[14] Škorc, G., Zapušek, S., Čas, J., Šafarič, R. (2010). Virtual user interface for the remote control of a nano-robotic cell using a haptic-device. *Strojniški vestnik – Journal of Mechanical Engineering*, vol. 56, no. 7-8, p. 423-435.

[15] Janot, A., Bidard, C., Gosselin, F., Gautier, M., Keller, D., Perrot, Y. (2007). Modeling and identification of a 3 DOF haptic interface. *Proceedings of Robotics and Automation, IEEE International Conference*, p. 4949-4955.

[16] Mali, U., Munih, M. (2006). HIFE-Haptic Interface for Finger Exercise. *IEEE/ASME Transactions on Mechatronics*, vol. 11, no. 1, p. 93-102, DOI:10.1109/TMECH.2005.863363.

[17] Baudendistel, K., Schad, R.L., Wenz, F., Essig, M., Schröder, J., Jahn, T., Knopp, V.M., Lorenz, J.W. (1996). Monitoring of task performance during functional magnetic resonance imaging of sensorimotor cortex at 1,5T. *Magnetic Resonance Imaging*, vol. 14, no.1, p. 51-58, DOI:10.1016/0730-725X(95)02052-U.

[18] Hartwig, V., Vanello, N., Gaeta, G., Sgambelluri, N., Scilingo, E.P., Bicchi, A. (2008). Design of fMRI Compatible Actuators. Retrieved at 2008-12-09, from *http://www.touch-hapsys.org/*.

[19] Klare, S., Peer, A., Buss, M. (2010). Development of a 3 DoF MR-compatible haptic interface for pointing and reaching movements. Haptics: Generating and Perceiving Tangible Sensations. *Lecture Notes in Computer Science 6192*, Springer-Verlag, Berlin Heidelberg, p. 211-218.

[20] Tsekos, N.V., Özcan, A., Christoforou, E. (2005). A prototype manipulator for magnetic resonance-guided interventions inside standard cylindrical magnetic resonance imaging scanners. *Journal of Biomechanical Engineering*, vol. 127, no. 6, p. 972-980, DOI:10.1115/1.2049339.

[21] Lee, S.S., Lee, M.J. (2003). Design of a general purpose 6-DOF haptic interface. *Mechatronics*, vol. 13, no. 7 p. 697-722, DOI:10.1016/S0957-4158(02)00038-7.

[22] Meneses, J., Castejón, C., Corral, E., Rubio, H., Garcia-Prada, J.C. (2011). Kinematics and dynamics of the quasi-passive biped "PASIBOT". *Strojniški vestnik – Journal of Mechanical Engineering*, vol. 57, no. 12, p. 879-887, DOI:10.5545/sv-jme.2010.210.

[23] Sudheer, A.P., Vijayakumar, R., Mohandas, K.P. (2011). Optimum Stable Gait Planning for an 8 Link Biped Robot Using Simulated Annealing. *International Journal of Simulation Modelling*, vol. 10, no. 4, p. 177-190, DOI:10.2507/IJSIMM10(4)2.186.

[24] Tsai, L.W. (1999). *Robot analysis, The Mechanics of Serial and Parallel Manipulators*. John Wiley & Sons, New York.

[25] Gosselin, F., Bidard, C., Brisset, J. (2005). Design of a high fidelity haptic device for telesurgery. *Proceedings of the IEEE International Conference on Robotics and Automation*. p. 205-210, DOI:10.1109/ROBOT.2005.1570120.

[26] Hayward, V., Oliver, R.A., Hernandez, M.C., Grant, D., Robles-De-La-Torre, G. (2004). Haptic interfaces and devices. *Sensor Review*, vol. 24, no. 1, p. 16-29, DOI:10.1108/02602280410515770.

[27] Yoshikawa, T. (1985). Manipulability of robotic mechanisms. Hanafusa, H., Inoue, H. (eds.): *Proceedings of Robotic Research: the 2nd International Symposium*, p. 439-446().

[28] Rajh, M., Glodež, S., Flašker, J., Gotlih, K., Kostanjevec, T. (2011). Design and analysis of an fMRI compatible haptic robot. *Robotics and Computer-Integrated Manufacturing*, vol. 27, no. 2, p. 267-275, DOI:10.1016/j.rcim.2010.06.007.

[29] Chiu, S.L. (1988). Task compatibility of manipulator postures. *The International Journal of Robotic Research*, vol. 7, no. 5, p. 13-21, DOI:10.1177/027836498800700502.

[30] Gotlih, K., Kovač, D., Vuherer, T., Brezovnik, S., Brezočnik, M., Zver, A. (2011). Velocity anisotropy of an industrial robot. *Robotics and Computer-Integrated Manufacturing,* vol. 27, no. 1, p. 205-211, DOI:10.1016/j.rcim.2010.07.010.

[31] Fonseca Ferreira, N.M., Tenreiro Machado, J.A. (2008). Manipulability analysis of two-arm robotic system, retrieved at 2008-12-19, from *http://ave.dee.isep.ipp.pt/~gris/_private/Nuno_INES00.PDF*.